International Journal of Biological Macromolecules 179 (2021) 279–291

Contents lists available at ScienceDirect

International Journal of Biological Macromolecules

journal homepage: http://www.elsevier.com/locate/ijbiomac

Lscβ and lscγ, two novel levansucrases of *Pseudomonas syringae* pv. actinidiae biovar 3, the causal agent of bacterial canker of kiwifruit, show different enzymatic properties

Simone Luti [a,*], Sara Campigli [b], Francesco Ranaldi [a], Paolo Paoli [a], Luigia Pazzagli [a], Guido Marchi [b]

[a] Department of Experimental and Clinical Biomedical Sciences, University of Florence, Italy
[b] Department of Agriculture, Food, Environment and Forestry, University of Florence, Italy

ARTICLE INFO

Article history:
Received 11 January 2021
Received in revised form 21 February 2021
Accepted 25 February 2021
Available online 03 March 2021

Keywords:
Levansucrase
Levan
Pseudomonas syringae
Plant pathogen
Sucrose
Actinidia spp.

ABSTRACT

Bacterial canker disease caused by *Pseudomonas syringae* pv. actinidiae (Psa) biovar 3 involved all global interest since 2008. We have found that in Psa3 genome, similarly to other *P. syringae*, there are three putative genes, *lscα*, *lscβ* and *lscγ*, coding for levansucrases. These enzymes, breaking the sucrose moiety and releasing glucose can synthetize the fructose polymer levan, a hexopolysaccharide that is well known to be part of the survival strategies of many different bacteria. Considering *lscα* non-coding because of a premature stop codon, in the present work we cloned and expressed the two putatively functional levansucrases of Psa3, lscβ and lscγ, in *E. coli* and characterized their biochemical properties such as optimum of pH, temperature and ionic strength. Interestingly, we found completely different behaviour for both sucrose splitting activity and levan synthesis between the two proteins; lscγ polymerizes levan quickly at pH 5.0 while lscβ has great sucrose hydrolysis activity at pH 7.0. Moreover, we demonstrated that at least *in vitro* conditions, they are differentially expressed suggesting two distinct roles in the physiology of the bacterium.

1. Introduction

Within the highly diverse group of Gram-negative bacteria known as the *Pseudomonas syringae* species complex (Pssc) [1], *Pseudomonas syringae* pv. actinidiae (Psa) is the causative agent of canker disease of kiwifruit, among which *Actinidia chinensis* var. deliciosa and *A. chinensis* var. chinensis are the major hosts (https://gd.eppo.int/taxon/PSDMAK). Production of kiwifruit is increasing because of consumer demand for its good taste and nutrition, but outbreaks of this bacterial disease often result in sudden and severe economic losses and limitations in kiwifruit cultivation worldwide [2].

Based on genetic diversity and toxins production [2–4] Psa has been categorized into six biovars (biovars 1–6). However, recently biovar 4 has been transferred to another pathovar, actinidifoliorum (Pfm) [5]. Whole genome comparisons have clearly shown that biovar 1 (Psa1), biovar 2 (Psa2) and biovar 3 (Psa3) are genetically distinct lineages of the same source population, each responsible of an independent outbreak. Outbreaks caused by Psa1 and Psa2 have remained geographically limited to Japan and Korea, respectively, but the expansion of Psa3, that has started at the end of last decade possibly in Italy, has now reached kiwi orchards worldwide, leading to what is currently referred to as the bacterial canker pandemy [6,7]. Moreover the same type of comparisons have pointed out a differential distribution of genes putatively coding for pathogenicity and virulence factors, that could possibly account for the higher agressivity of Psa3 respect to biovars 1 and 2 [7,8]. More recently, studying gene expression of Psa3 during the late stages of kiwi plantlets infection or in response to exposure to antimicrobial compounds, it has been observed, among the rest, an increase of the expression of genes coding for the exopolysaccharide (EPS) alginate [9–11]. *P. syringae* produces two major EPSs: alginate and levan. However, meanwhile it is well documented that alginate contributes both to the epiphytic fitness and to virulence of *P. syringae*, much lesser is known about the functions of levan [12–15]. Levan is non-structural EPS produced by many microbes including *Archaea*, fungi and a wide range of bacteria but only rarely by plants [16]. It is composed of fructose units connected predominantly by β-(2–6) linkages with some β-(2,1) branching points. In bacteria it is believed that levan constitutes a form of energy storage, or an important structural component of some bacterial biofilms, matrices that embed cells *in vitro* and *in vivo*, and which are composed also by proteins, lipids and nucleic acids thus playing a major role in the survival of bacteria [17]. Most interestingly however, this is not true for *P. syringae*, for which it has been proven that levan, as well as alginate, has only a marginal role in the architectural form of the biofilm [18]. Nevertheless levan it might be particularly important during early stages of infection

* Corresponding author at: viale Morgagni 50, 50134 Florence, Italy.
E-mail address: simone.luti@unifi.it (S. Luti).

https://doi.org/10.1016/j.ijbiomac.2021.02.189
0141-8130/

by masking and protecting the pathogen from the detection and defence mechanisms of the host, as it has been proposed to be the case for *P. syringae* pv. phaseolicola [19]. Moreover, some observations using a levan deficient mutant of *P. syringae* pv. glycinea PG4180, have suggested a decrease in the epiphytic survival, multiplication and symptoms induction when the mutant is spray inoculated on soybean plants as compared to the wild type parental strain [20]. In *Pseudomonas* levan is synthesized by bacterial extracellular enzymes levansucrases (lsc) (EC 2.4.1.10), whose mechanism involve the breakage of the glycosidic linkage in the sucrose molecule, resulting in the formation of a covalent fructosyl-enzyme intermediate and the release of the glucose moiety. The fructosyl moiety is then transferred from the enzyme to an acceptor molecule; as a result, the acceptor is elongated in one fructosyl unit (polymerization). When a water molecule acts as acceptor of the fructosyl intermediate, fructose is released into the reaction media (hydrolysis) [16]. Interestingly, meanwhile most bacteria species harbour a unique lsc coding gene, the members of Pssc, possess up to three. An explanation for the occurrence of multiple *lsc* copies is yet to be found [1,16,21].

To date the best characterized lscs of *Pseudomonas* are lsc1, lsc2 and lsc3 from *Psudomonas syringae* pv tomato DC3000 [22] and lscA, lscB and lscC from *P. syringae* pv. glycinea PG4180 [20]. *LscA/2* is usually present in a single copy in *P. syringae* genomes but its variants have been found in other enterobacteriaceae, including the phytopathogenic species *Erwinia amylovora*, leading to the hypothesis that it has been exchanged by HGT (Horizontal Gene Transfer) among genera [21]. On the contrary the other two levansucrase coding genes *lscB/1* and *lscC/3*, have been reported to occur only in *P. syringae* pathovars. In DC3000 they share a sequence identity of 95% both at nucleotide and amino acidic level, meanwhile in PG4180 they share a sequence identity of 98% and 99% at nucleotidic and amino acidic levels, respectively, and are referred to as "variant BC alleles" [21]. Mutagenesis experiments of lsc2 and lsc3 demonstrate that Asp62, Asp219 and Glu303 are the crucial amino acids for activity: in the active site they form the catalytic triad in which Asp62 acts as nucleophile, Glu303 as acid/base catalyst and Asp219 as stabilizer [23]. Other amino acids besides the catalytic triad are important for lsc, therefore studying their impact could be very important to lay the basis for a functional characterization of these enzymes [24,25]. In addition, other factors such as temperature, substrate or enzyme concentration and the presence of solvents or salts can modify their activity. For several lscs of *Pseudomonas* bacteria the pH optima are rather similar and close to 6.0 even if in some cases their activity shows pH fluctuation [23,26]. Finally, they are resistant to high temperature confirming their great stability as to be expected for bacterial extracellular enzymes [23,27].

This work starts from the comparison of the *lsc* genes sequences reported in the NCBI databases: according to which the gene NZ708_RS29580, putatively codes for a plasmidic lsc of Psa3 strain ICMP 18708. If it is functional, it would possess a 45 nucleotide region at the 5′ end that would render it unique not only respect to the homologous genes of the other Psa biovars (and Pfm), but within the Pssc.

Since levan production, size and structure could be important also for pathogenesis and knowing the role of the different lscs present in Psa3 could be crucial for understanding its great virulence, by cloning and expressing two new *lsc* genes from Psa3 in *E. coli*, aim of the present study was to determine for the first time if they produce functional protein products as well as their optimum of activity and kinetic parameters in different conditions.

2. Materials and methods

2.1. Nucleotide sequence analysis and comparison

Strain KL103 was isolated from a kiwi leaf on KBC semi-selective medium [28] and characterized as Psa3 according to the LOPAT determinative scheme [29] and by MLSA sequencing four housekeeping gene fragments *pfk*, *rpoD*, *cts* and *pgi* following the procedures for DNA extraction, PCR amplification and direct sequencing as previously described [3].

Database searches were carried out using BLAST algorithms available on the National Center for Biotechnology Information (NCBI, http://www.ncbi.nlm.nih.gov) using the nucleotide sequences of the *lscA* (AF037443), *lscB* (AF345638) and *lscC* (AF346402) levansucrase coding sequences of *P. glycinea* PG4180 as query. The homologous sequences of the 3 selected genes including their flanking regions, of complete genomes of *Pseudomonas syringae* pv. actinidiae: eight biovar 3, one biovar 1 (Psa1), one biovar 5 (Psa5), were retrieved and aligned using Muscle multiple sequence alignment tool to estimate intra and inter pathovars similarities (implemented in Mega X [30]). To obtain the corresponding sequences from Psa3 KL103, primers listed in Table S1 were designed. To amplify the KL103 putative *lsc* genes (*lscα*, *lscβ*, *lscγ*), reagent mix composition was: 1× PCR buffer (New England BioLabs), 0.2 mM each dNTP (Thermo Scientific), 1.25 U of Q5 Hot Start High-Fidelity DNA Polymerase (New England BioLabs), 0.2 μM of each primer and 50 ng of template DNA. Thermal cycling consisted of 3 min at 95 °C for initial denaturation, 35 cycles of denaturation at 95 °C for 30 s, annealing at 62 °C for 30 s, extension at 72 °C for 2 min, followed by 10 min at 72 °C for final extension. All PCR products obtained from Psa3 KL103 were purified using ExoSAP-IT (Usb Corporation) according to the manufacturer's protocol and subjected to direct sequencing. Nucleotide sequences were visualized using CHROMAS LITE 2.01 (Technelysium) and identity searches were performed using software tools BlastN and BlastP available from the NCBI. *lsc* nucleotide sequences were aligned using MUSCLE and a cladogram was constructed (1235 positions in the final dataset) using the Neighbor-Joining method and the Kimura 2 parameter model of evolution.

2.2. lscγ mRNA analysis

A preliminary trial was performed to check if *lscγ* gene is actually expressed in Psa3 KL103. The strain was grown in 100 mL of NB or NB with 5% (w/v) sucrose (NBS) at 25 °C, 200 rpm, for 72 h. At different time point (24 h, 48 h and 72 h), 1 mL of culture was centrifuged at 10,000*g* for 2 min and pellet subjected to total RNA extraction by NucleoZOL (MACHEREY-NAGEL) following manufacturer instruction. Final RNA pellet was recovered by 50 μL of nuclease free water and it was subsequently subjected to nucleic acid quantification through Nanodrop spectrophotometer ND-1000. Total RNA (18 μg) was DNase (MACHEREY-NAGEL, rDNase, 740963) treated and reverse transcribed by RevertAid First Strand cDNA Synthesis Kit (Thermo Scientific) using oligo(dT). cDNAs, were PCR amplified (DreamTaq, Thermo Scientific) using primers plasmL1/R1 (Table S1) with the following procedure: 2 min at 94 °C for initial denaturation, 40 cycles of denaturation at 94 °C for 30 s, annealing at 62 °C for 30 s, extension at 72 °C for 1 min, followed by 5 min at 72 °C for final extension. PCR products were visualized on 1.3% (w/v) agarose gel. DNAse-treated RNA was used as control for DNA contaminations.

2.3. Lscβ and lscγ cloning in pGEM-T and E. coli 5α

The coding regions of *lscβ* and *lscγ* sequences and ~100 bp of 5′ and 3′ noncoding sequences were PCR-amplified from lysed cells of Psa3 KL103 using primers reported in Table S1. PCR products were purified from agarose gel troughs QIAquick Gel Extraction Kit (QIAGEN) and then cloned in pGEM-T vector using the pGEM®-T Easy Vector Systems (PROMEGA) following the manufacture instructions. Finally, plasmids were used to transform the 5-alpha competent *E. coli* cells (New England BioLabs) and colonies were selected with blue/white screening and standard ampicillin selection. Correct DNA insertion was checked by sequencing using primers T7/SP6.

2.4. Lscβ and lscγ cloning in pNIC28 and E. coli BL21

Using ligation-independent cloning (LIC) and primers reported in Table S1, the *lscβ* and *lscγ* genes derived from the previously obtained pGEM plasmids, were cloned in pNIC28-Bsa4 systems as reported by Vega et al. [31].

Obtained recombinant plasmids were used to transform 5-alpha competent *E. coli* cells and colonies from LB agar plates, supplemented with 50 μg/mL kanamycin and 5% (w/v) sucrose, were cultured, and plasmid purification was performed using the NucleoSpin plasmid extraction kit (MACHEREY-NAGEL). Transformants were characterized by colony PCR screening using the primers for the inserts and the correct nucleotide sequences were verified by DNA sequencing. Purified plasmids were than used to transform *E. coli* BL21 (DE3) cells (New England Biolabs).

2.5. Production, purification, and characterization of recombinant levansucrases

2.5.1. Production and purification

Expression and purification of recombinant lscβ and lscγ were performed in the same manner. *E. coli* BL21 cells were grown at 37 °C under shaking in 1 L of LB broth with 50 μg/mL kanamycin; at $O.D._{600} = 0.6$. Proteins expression was induced by 0.4 mM IPTG for 20 h at 18 °C. Then cells were centrifuged at 2000*g* for 20 min and pellets were resuspended in 40 mL of 50 mM sodium phosphate buffer pH 6.0, 300 mM NaCl, 10% (v/v) glycerol and 10 mM imidazole (Buffer A) [22]. Bacterial cells were harvested by 5 sonication steps of 30 s at 50 kHz and centrifuged again at 13,000*g* for 25 min at 4 °C.

lscβ and lscγ were purified from the whole cell lysate by IMAC Sepharose High Performance (Ge Healthcare) charged with Ni^{2+}.

The lysate (40 mL) was applied to a 10 mL Ni^{2+}-resin in a gravity column equilibrated with buffer A. The column was washed with buffer A with 25 mM imidazole and then eluted with buffer A with 250 mM imidazole and the pooled fractions were concentrated to 5 mL for TEV (Tobacco Etch Virus protease) treatment to remove the 6His-tag.TEV treatment was performed at 37 °C in 50 mM Tris/HCl pH 8, 10% (v/v) glycerol for 20 h. Subsequently, sample were applied again on Ni^{2+}-resin in a gravity column for un-catted and tag removing. Finally, lscs were further purified by gel chromatography on a HiLoad 16/600 Superdex 200 pg column driven by an Akta Pure 25 L system (GE Healthcare, Waukesha, WI, USA) at a flowrate of 1 mL/min and they were step eluted with 50 mM Tris/HCl pH 8.0 and 300 mM NaCl. Proteins were collected (50 fractions, 2 mL each), and analysed by SDS-PAGE, using 4–20% Mini-Protean TGX Precast polyacrylamide gels (Bio-Rad, Hercules, CA, USA).

2.5.2. Mass spectrometry analysis

Mass spectrometry analysis were performed by Mass Spectrometry Center (CISM) of Florence University as reported in Vega et al., 2019 using chymotrypsin as protease.

2.5.3. Protein quantitation

Proteins quantitation were performed by bicinchoninic acid method (BCA, Pierce Chemical, Rockford, IL) using BSA as protein standard.

2.5.4. Analytical gel-filtration

Analytical gel-filtration was carried out as reported in Vega et al. [31] with slight modifications. Briefly, lscs samples and standard proteins of know molecular weight (thyroglobulin 669 kDa, apoferritin 443 kDa, alcohol dehydrogenase 150 kDa, BSA 66 kDa, carbonic anhydrase 29 kDa and a-lactalbumin 14 kDa) were loaded in a Superdex 200 Increase 10/300 GL column (GE Healthcare) equilibrated with Tris/HCl pH 8.0, NaCl 300 mM buffer at 4 °C and run by Akta Pure 25 L. Elution volumes were taken as the volumes of buffer passed through the column between sample injection and the point of highest absorbance. A plot of elution volume *vs.* log[MW] (data not shown) was obtained with the standards data points and fitted to a linear regression curve [32]. The elution volumes measured for both the lscs were then interpolated into the resulting standard curve to obtain the corresponding MW.

2.5.5. Dynamic light scattering

Size distribution analysis was performed at 25 °C with a Malvern Zetasizer Nano S Dynamic Light Scattering (DLS) device (Malvern Panalytical, Malvern, United Kingdom) using proteins at a concentration of 0.5 mg/mL in 50 mM Bis/Tris pH 7.0 buffer. Each sample was centrifuged at 13,000*g* for 15 min at 4 °C, filtered with Whatman Anotop 0.02 μm cut-off filters (Millipore Sigma), and analysed considering the refraction index and viscosity of the dispersant. A 10-mm reduced volume plastic cell was used.

2.5.6. CD spectra

Analysis was performed at 1 mg/mL of proteins in 12.5 mM Tris/HCl pH 8.0, NaCl 20 mM. CD spectra were recorded in the far-UV region from 190 to 260 nm using a JASCO J-810 spectropolarimeter (Tokyo, Japan). The spectra were acquired using a 0.1 mm path length quartz cell, a band width of 1 nm, a response time of 0.5 s, a data pitch of 0.5 nm and a scanning speed of 20 nm/min. Each spectrum was the average of 16 consecutive scans followed by subtraction of the blank spectra.

2.5.7. Differential scanning fluorimetry

Differential scanning fluorimetry (DSF) was performed using a Bio-Rad CFX96 (Biorad) by selecting the FAM (FRET) filter. Analysis was performed with 0.1 mg/mL of protein and 1:500 of SYPRO Orange (ThermoFisher Scientific, Waltham, MA, USA) in 50 mM Sodium Acetate pH 5.0 or 50 mM Bis/Tris pH 7.0 buffers in a final volume of 25 μL. All samples were prepared in triplicate. The samples where heated with a ramp speed, which provides a 2 min pause at 25 °C, followed by a ramp to 95 °C, increasing the temperature of 1 °C/min. The SYPRO Orange fluorescence was plotted *versus* temperature (melting curve) and the resulting plot converted into its first order derivative, which provided the melting temperature (Tm).

2.6. Sucrose hydrolysis activity of proteins

Sucrose hydrolysis activities of lscβ and lscγ were checked measuring the amount of glucose liberated during incubation with sucrose. There are several useful methods for glucose detection [33], between them we chose the DiNitroSalicylic acid (DNS) method because previously used in lsc reactions [22].

2.6.1. pH dependence

Experiments were performed at 0.03 μg/μL enzymes concentration with 150 mM sucrose in buffer at different pH. Total volume assays were 100 μL and the total ionic strength of each buffer were 100 mM. Used buffer: pH 4.0 and 5.0 50 mM sodium acetate; pH 6.0 and 7.0 50 mM Bis/Tris; pH 8.0 and 9.0 50 mM Tris. Reactions were conducted at 37 °C for 10 min and then stopped boiling samples. Finally, DNS method was used to determine the glucose.

2.6.2. Ionic strength dependence

Experiments were performed at 0.03 μg/μL enzymes concentration with 150 mM sucrose in 50 mM Bis/Tris pH 7.0 buffer. Different concentrations of NaCl were added to each tube starting from 0 to 1 M. Total analysis volume was 100 μL and tests were done at 37 °C for 10 min. After, reactions were stopped, and glucose concentrations were determined by DNS method.

2.6.3. Temperature dependence

Experiments were performed at 0.03 μg/μL enzymes concentration with 150 mM sucrose in a buffer 50 mM Bis/Tris pH 7.0, or 50 mM sodium acetate pH 5.0. Total analysis volume was 100 μL and tests were

done at 5 °C, 15 °C, 25 °C, 37 °C, 45 °C, 55 °C and 65 °C for 10 min. After, reactions were stopped, and glucose concentrations were determined by DNS method.

2.6.4. Km determinations

Experiments were performed at 0.1 μg/μL enzymes concentration with variable concentrations of sucrose in a buffer 50 mM Bis/Tris pH 7.0 or 50 mM sodium acetate pH 5.0, at 37 °C for 10 min. Reaction rate was determined for each assay and reported on Michaelis-Menten chart to determine K_m and V_{max}. k_{cat} were obtained using the following equation:

$$kcat = \frac{Vmax}{[E]tot}$$

where Vmax was the maximum velocity of the reaction and [E]tot was the total enzyme concentration.

2.6.5. DNS

Glucose concentration was determined by DNS method as reported by Goncalves et al. 2010 [34] with slight modifications. Briefly, reaction was carried out in 96 wells plate, adding 25 μL of DNS reagent to 25 μL of sample, or distilled water (blank). Subsequently, in order to perform the reaction, the microtiter plate, with cap, was placed at 95 °C for 10 min, then it was placed on ice and 250 μL of distilled water were immediately added to each well. Calibration curve was obtained starting from 0 to 250 μg of glucose. Finally, samples absorbances were read at 540 nm in a BioTek Synergy H1 Hybrid Multi-Mode Reader.

2.7. Polymerization activity of proteins

Levan synthesis kinetics was monitored in a turbidity assay on microtitre plate [22]. Reaction was performed at 37 °C in 200 μL of buffer at pH 5.0 (50 mM sodium acetate) or 7.0 (50 mM Bis/Tris), containing different concentrations of sucrose and 10 μg of purified levansucrases protein per mL of reaction mixture. Turbidity of the samples at 400 nm was recorded every 5 min using a BioTek Synergy H1 Hybrid Multi-Mode Reader.

2.8. Lscβ and lscγ expression analysis

Template-specific primers and probe were designed for *lscβ* and *lscγ* of Psa3 KL103 (Table S1) and the specificity of each set was verified against each other using 50 ng of purified pGEM plasmids containing the insert of interest. Strain KL103 was grown on nutrient agar plates at 25 °C for 72 h, resuspended in sterile distilled water at a concentration of approximately 3.6×10^5 cfu/mL ($OD_{600} = 0.07$) and 100 μL of the resulting suspension was used to inoculate 100 mL of NB. The culture was grown on a rotary shaker at 25 °C and 200 rpm for 10 days. At 0 h, 4 h,10 h, 12 h, 24 h, 36 h, 48 h, 72 h, 144 h and 240 h, pH and cells number were determined by plate count method, and RNA extracted from 0.5 mL of culture. For pH determination, 3 mL of culture were centrifuged at 12,000*g* for 5 min and supernatant analysed by pH meter.

RNA was extracted by NucleoZOL (MACHEREY-NAGEL) following the manufacturer instructions and quantified *via* Nanodrop spectrophotometer ND-1000 (Nanodrop). 600 ng of total RNAs were DNase treated (MACHEREY-NAGEL, rDNase, 740963) for 1 h at 37 °C and then, a RT-PCR was performed on 300 ng of DNAse treated-RNA using the RevertAid First Strand cDNA Synthesis Kit (Thermo Scientific) as recommended by the manufacturer. The gene specific *lscβ* and *lscγ* primers and probe were used to check for presence of mRNA by PCR using cDNA as template. DNAse-treated RNA was used as control for DNA contaminations.

Real-Time PCR was performed in a Biorad CFX96 instrument using the following thermocycler program: 1 cycle of 95 °C for 2 min; 40 cycles of 95 °C for 15 s and 62 °C for 1 min. Each sample was run in triplicate using GoTaq® Probe qPCR Master-mix (Promega), and primers and TaqMan probe sets are reported in Table S1. Reaction volume was 15 μL.

2.8.1. Absolute quantification real-time PCR assays

pGEM-*lscβ* and pGEM-*lscγ* plasmids were used to build a standard curve for absolute mRNA quantifications for the expression analysis of the two levansucrases. 20 ng of circular plasmids were linearized with *BSAI* (NEB) restriction enzyme following manufacturer instructions and used to build an eight point standard curve ranging from 16 ng to 0.16 fg. 15 μL reactions for all standards were run in triplicate under the same conditions of samples. Average Ct values and log (ng) values were used to obtain a linear regression equation allowing for calculation of ng of cDNAs of *lscβ* and *lscγ* in Psa3 KL103 [35].

3. Results

3.1. Nucleotide sequence analysis and comparison

All Psa3 complete genomes considered in this study as well as Psa1 ICMP 9853, possess 3 putative *lsc* coding genes. Invariably in Psa3, two lscs are chromosome located (*lscα* and *lscβ*) meanwhile one is plasmid borne (*lscγ*). On the contrary, strain MAFF212063 (Psa5) possess only two putative *lsc* coding genes which are both on the chromosome. When tested for presence of the *lscα* gene sequence, the expected amplicon was yield from strain Psa3 KL103 DNA and its length was 1248 bp. The nucleotide sequence showed 87% identity with *P. syringae* pv. glycinea PG4180, 99% with Psa1 (ICMP 9853), Psa2 (ICMP19072) Psa5 (MAFF212063) and *P. syringae* pv. *actinidifoliorum* (CFBP8039), and 100% with all Psa3 whole genomes considered in this study (data not shown). Noticeably, in all Psa3 homologous sequences, a G to A transition was found 187 bp downstream of the translation initiation codon of this gene and *in silico* analyses indicated that the deriving nucleotide mutation would generate an early termination codon implying that this gene is most likely not functional in Psa3 (Fig. S1). In accordance with Psa3 complete genomes, the two others predicted *lsc* genes were isolated from strain KL103 by PCR, and their translated sequence encodes for proteins of 431(WP_017684964) (hereafter called lscβ) and 430 (WP_017685048) (called lscγ) amino acidic residues, respectively. lscβ, whose genetic determinant is chromosome located in all Psa3 genomes, shares 98% identities with either lscB or lscC of PG4180 which however are 99% identical one to each other. On the contrary the first 14 predicted amino acid residues located at the putative N-terminus of the lscγ protein (MIAGRRHFDCRPLH) appear to be unique. The genetic determinant of lscγ is on a large plasmid (74,432 bp, p18708 in Psa3 ICMP18708; [36]) carried by all Psa3 and the first 14 N-terminal aminoacids of the encoded protein are different not only from the corresponding N-terminal domain of lscβ (Fig. 1) but also from that of other Psa as well as *P. syringae* levansucrases annotated in the prok_complete_genomes database (data not shown). Using BLAST we searched for the presence of signal peptide consensus sequence against the NCBI's non-redundant (NR) protein database but no significant score was obtained (data not shown). It is noteworthy that despite its localization on mobile genetic element, *lscγ* coding gene is highly conserved without any sequence variation in all Psa3 complete genomes. The predicted catalytic motifs I, II and III of PG4180 BC variants were found in both lscβ and lscγ proteins (Fig. 1).

3.2. Search of lscγ mRNA presence in Psa3

Aimed to verify if the *lscγ* gene (NZ708_RS29580) was expressed in Psa3, bacteria were grown on NB and NBS for 72 h and then checked for the presence of the mRNA. *lscγ* specific primers produced a 231 nucleotide fragment from cDNA, and Sanger sequencing results confirmed the identity both when Psa3 KL103 was grown on NB or NBS (data not

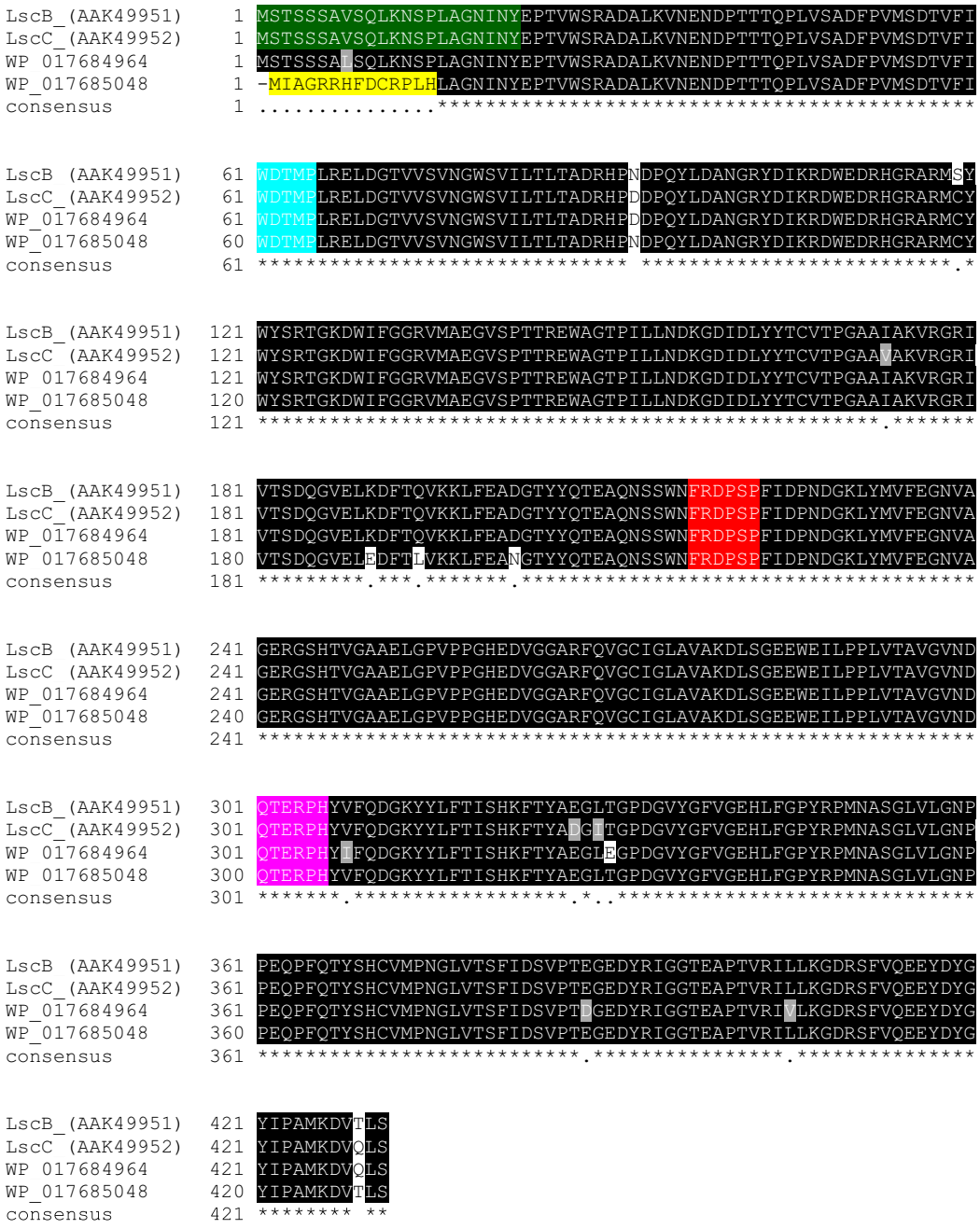

Fig. 1. Alignment of the predicted amino acid sequence of levansucrases: amino acid sequences of WP_017684964 (lscβ, chromosome encoded) and WP_017685048 (lscγ, plasmid pM228 encoded) of strain Shanxii 228 of *P. syringae* pv. actinidiae biovar 3. The lscB (AAK49951) and lscC (AAK49952) levansucrase enzymes sequences of *Pseudomonas syringae* pv. glycinea strain PG4180 were also aligned for comparative purposes. The predicted N-terminal sequence of lscB and lscC is highlighted in green [20]; the predicted catalytic motifs I, II and III are highlighted in blue, red and purple respectively [21]. The first 14 aa at the N-terminal of WP_017685048 are highlighted in yellow. (For interpretation of the references to color in this figure legend, the reader is referred to the web version of this article.)

shown). Thus, this gene was effectively transcripted by the bacterium both in presence and absence of sucrose in the medium.

3.3. Cloning of *lscβ* and *lscγ* genes

lscβ and *lscγ* gene were cloned in the pNIC28 expression system and recombinants were produced in *E. coli* BL21 as described in experimental procedures.

To check the ability of cloned genes to produce levan, the BL21 pNIC28-*lscβ*, BL21 pNIC28-*lscγ* and BL21 wild type cells were plated in LB agar with 5% sucrose. Bacteria were grown for 24 h at 37 °C and then at 4 °C for 48 h. After 72 h, BL21 cells with recombinant levansucrase showed the typical colony shape of levan positive bacteria but not the wild type BL21, suggesting the correct functionality of both lscγ e lscβ enzymes (Fig. 2).

3.4. Expression and structural characterization of recombinant levansucrases from Psa

Recombinant lscβ and lscγ proteins were obtained through the same purification procedure. Briefly, the 6His-tagged proteins were recovered after bacterial lysis and purified by Ni^{2+}-affinity column. Tag was deleted from proteins by enzymatic cleavage by TEV (Tobacco Etch Virus protease) and removed through another passage in Ni^{2+}-

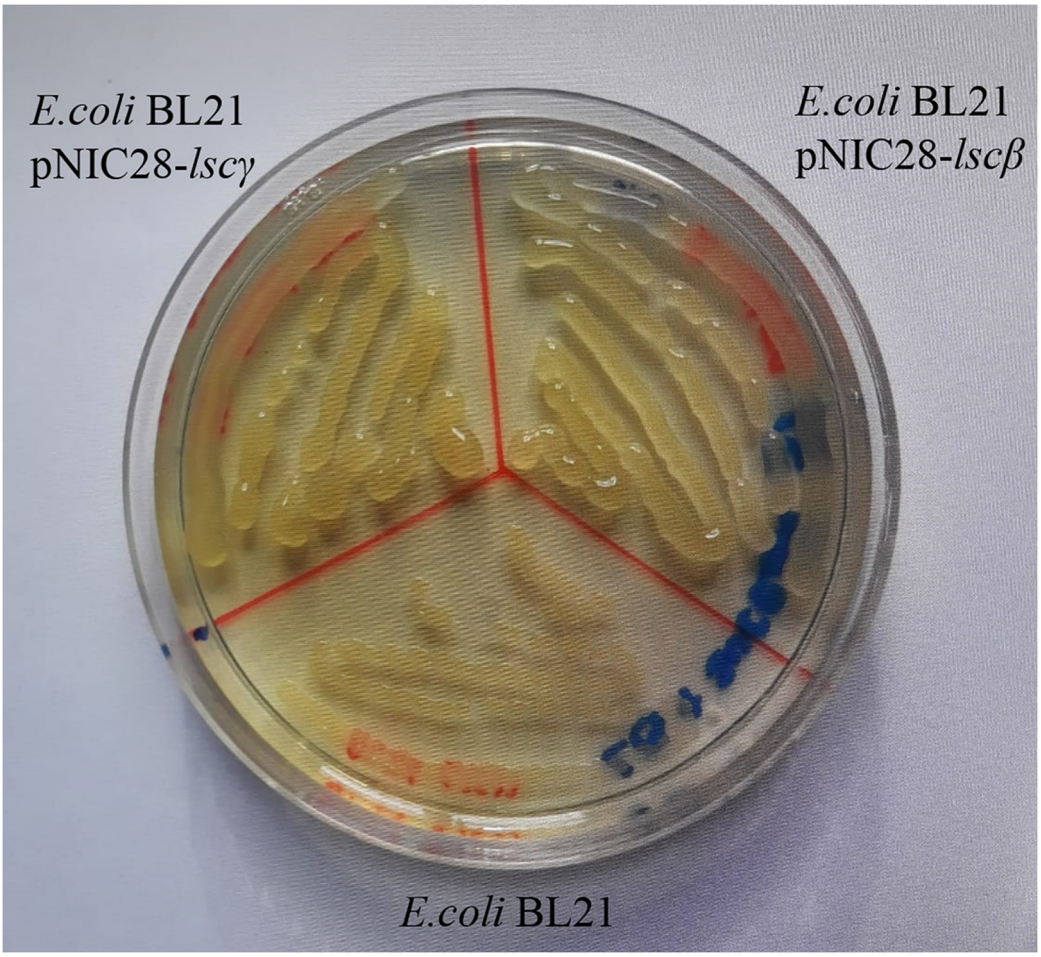

Fig. 2. *E. coli* BL21 strains with recombinant lscβ and lscγ produce levan: BL21 pNIC28-*lscβ*, BL21 pNIC28-*lscγ* and BL21 only cells on LB agar with 5% sucrose. Bacteria were grown for 24 h at 37 °C and then at 4 °C for 48 h. BL21 pNIC28-*lscβ*, BL21 pNIC28-*lscγ* showed the typical colony shape of levan positive bacteria while wild type BL21 not.

affinity column. Finally, proteins were further purified by size exclusion column. The purification procedure allowed to obtain 80 mg and 50 mg of pure protein for lscβ and lscγ, respectively.

Proteins purity and molecular weight were checked by SDS-PAGE (Fig. S2) and further confirmed by mass spectrometry analysis (Fig. S3). Proteins were digested with chymotrypsin which permitted the identification of several protein fragments that were assigned to portions of the sequences, validating the identity of the two proteins (Fig. S3a). The amino acid sequences of lscβ and lscγ is very similar and the main differences are at the N-terminal regions (Fig. 1). Although the fragments obtained after chymotrypsin digestion did not cover the N-terminus, the different fragmentations allowed to distinguish the two proteins (Fig. S3b).

Some studies reported that lsc could be found in dimeric or monomeric form [37]. In order to analyse the proteins behaviour in solution, we estimate the molecular weight of the particles by analytical Gel Filtration. Fig. 3a showed the chromatogram of the two proteins at pH 7.0 which presented similar elution volume, indicating that the two proteins were in the same form.

A calibration curve was obtained by plotting the elution volumes of 6 known proteins *vs* their MW in logarithmic form (data not shown). This allows us to estimate the MW of lscβ and lscγ which results 85.8 ± 4.8 and 86.6 ± 6.3 kDa, respectively. Because the MW of each lscβ and lscγ monomer is 47.6 kDa, this apparent MW is consistent with a dimer. The ability of proteins to form functional dimers was confirmed by dynamic light scattering (DLS) analysis (Fig. 3b). The hydrodynamic diameter of the two proteins was similar and compatible with the dimeric form of the proteins (lscβ 8.7 ± 1 Å lscγ and 10.1 ± 1 Å).

To further characterize lscβ and lscγ, far-UV-CD spectra of the proteins were obtained (Fig. 3c). They were very similar and presented the analogue shape of other lscs from Gram negative bacteria [38]. We performed the deconvolution of these spectra using the BeStSel algorithm (http://bestsel.elte.hu) obtaining the 45% and 46% of β-sheets for lscβ and lscγ, respectively (data not shown), confirming the probable five-bladed β-propeller architecture characteristic of many lscs [24].

Another typical feature of lscs is the high stability; in fact, they are extracellular proteins subjected to constant stress, such as changing in pH, salt and temperature and they needed to be stable for a correct function [23]. Therefore, stability of lscβ and lscγ was determined by DSF, which allows the rapid and sensitive assessment of protein thermal stability. Using Sypro-orange we were able to determine the T_m of proteins calculating the first derivative of DSF curve obtained (Fig. 3d). Our data revealed that lscβ and lscγ had a Tm respectively of 60.0 ± 0.0 °C and 55 ± 0.0 °C, confirming the high thermal stability of lscs [23].

Finally, through the Expasy SWISS-MODEL tools (https://swissmodel.expasy.org/interactive), which use a comparative approach to generate 3D models of a protein, we obtained a 3D models of both lscβ and lscγ which appear quite similar to each other and to other lscs (Fig. S4).

3.5. Sucrose hydrolysis activity of lscβ and lscγ

The sucrose splitting activity was performed using 0.63 μM of enzymes (lscβ and lscγ), and 150 mM sucrose and incubation time of 10 min.

Firstly, the effect of pH on enzymatic activity was investigated. Both lsc enzymes show the maximal activity in the 5–7 pH range, while the activity of enzymes decreases at pH values lower that 5 and higher

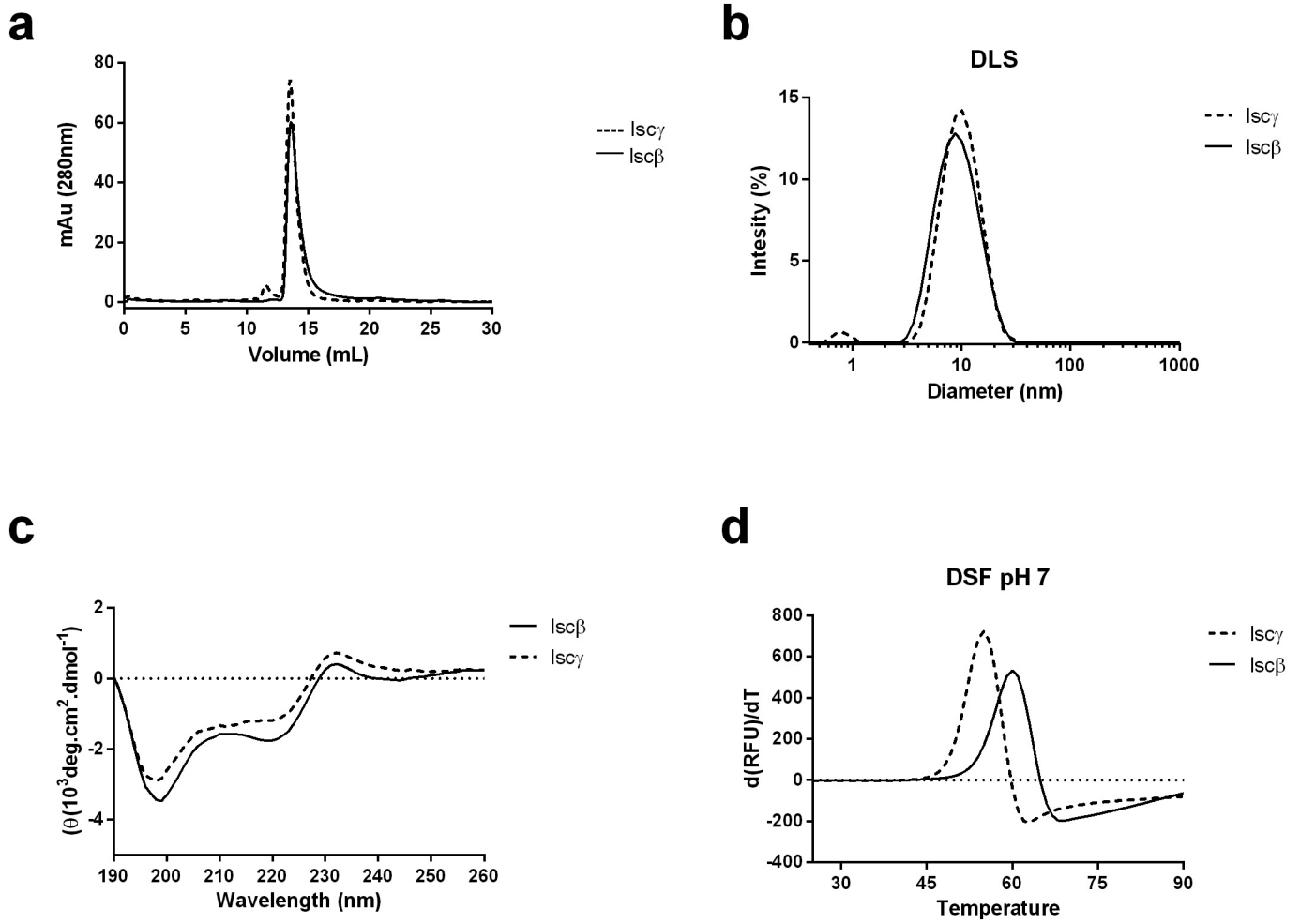

Fig. 3. Structural characterization of lscβ and lscγ: a) Analytical gel filtration of the proteins. The chromatogram shows a protein peak at 13.3 mL of elution volume. AU, arbitrary units. b) Particle size distributions of lscβ and lscγ at pH 7.0. c) CD spectra of proteins at 0.1 mg/mL concentration. d) First derivative of DSF measurements of lscβ and lscγ at 0.1 mg/mL concentration using Sypro orange as environmentally sensitive dye.

than 8 (Fig. 4a). Interestingly, we found that at pH 7.0 the activity of lscβ increase over lscγ, reaching a hydrolysis rate twice than that of lscγ (299.5 ± 26.7 μg glucose x min^{-1} of lscβ respect to 170 ± 10.6 mg glucose x min^{-1} of lscγ), indicating that the influence of pH on the hydrolytic activity of lscβ is considerably more pronounced respect to lscγ.

The optimum ionic strength for enzymatic activity was detected by incubating both enzymes at pH 7.0, in the presence of increasing salt concentrations. Indeed, the activity of both lscβ and lscγ (Fig. 4b) was negatively affected by salt concentration, even if lscβ activity decreases more sharply than that of lscγ. This finding suggests that the activity of these enzymes is differently influenced by ionic strength [39].

Finally, the dependence of enzymes activity by temperature was measured. The hydrolysis rate of lscβ and lscγ at two different pH values was analysed: (i) at pH 5.0, a value at which the enzymes work in a similar manner, and (ii) at pH 7.0, a condition in which the two proteins showed a different activity. Our results confirmed that at pH 5.0 (Fig. 4c) the dependence of lscβ and lscγ activity from temperature is very similar. Indeed, the activity of both enzymes progressively increases with temperature until 55 °C, and then fall quickly, suggesting that temperatures higher than 55 °C induce denaturation of both enzymes (Fig. 4c).

Interestingly, the trends of the two proteins were completely different at pH 7.0 (Fig. 4d). In fact, meanwhile lscγ behaved in the same manner observed at pH 5.0, the activity of lscβ increases rapidly passing from 4 to 15 °C and remains constant up to 55 °C. Thus, at pH 7.0 the activity of lscγ is strongly influenced by the temperature, but the activity of lscβ remains unchanged in a wide temperature range. Moreover, in all the tested conditions, both enzymes dramatically loosed the activity at 65 °C, thereby undergoing to denaturation (Fig. 4d). Overall results obtained on lscβ and lscγ hydrolysis rates highlight their different behaviour, and suggest that these two enzymes are differentially susceptible to environmental changes.

With the aim of further investigating the different activities of lscβ and lscγ the main kinetic parameters of the enzymes were measured. It has been reported that lsc exhibit Michaelis-Menten kinetic properties for both the hydrolase and transferase activities [16], so we used this approach to calculate the K_m and k_{cat} of the enzymes. We observed that pH did not affects kinetic activity of lscγ (Fig. 5a); in fact this enzyme shows the same K_m and V_{max} values at pH 5.0 and 7.0 (Table 1). Similarly, at pH 5.0 kinetic parameters of lscβ are very close to that of lscγ, even if these changes sharply moving from pH 5.0 to pH 7.0, showing a lower substrate affinity but a higher k_{cat} value (Fig. 5b and Table 1). Interestingly, despite these changes the specificity constant (k_{cat}/K_m) does not change, suggesting that the impairment of affinity for substrate (sucrose) is compensated by an enhanced hydrolysis rate. This finding suggests that the shift of pH is related with a change in protonation status of a catalytic residue [26].

3.6. Polymerization activity of proteins

Time course synthesis of levan by lscβ and lscγ was studied. Turbidity assay were performed on microplates in buffer at pH 5.0 or 7.0, at

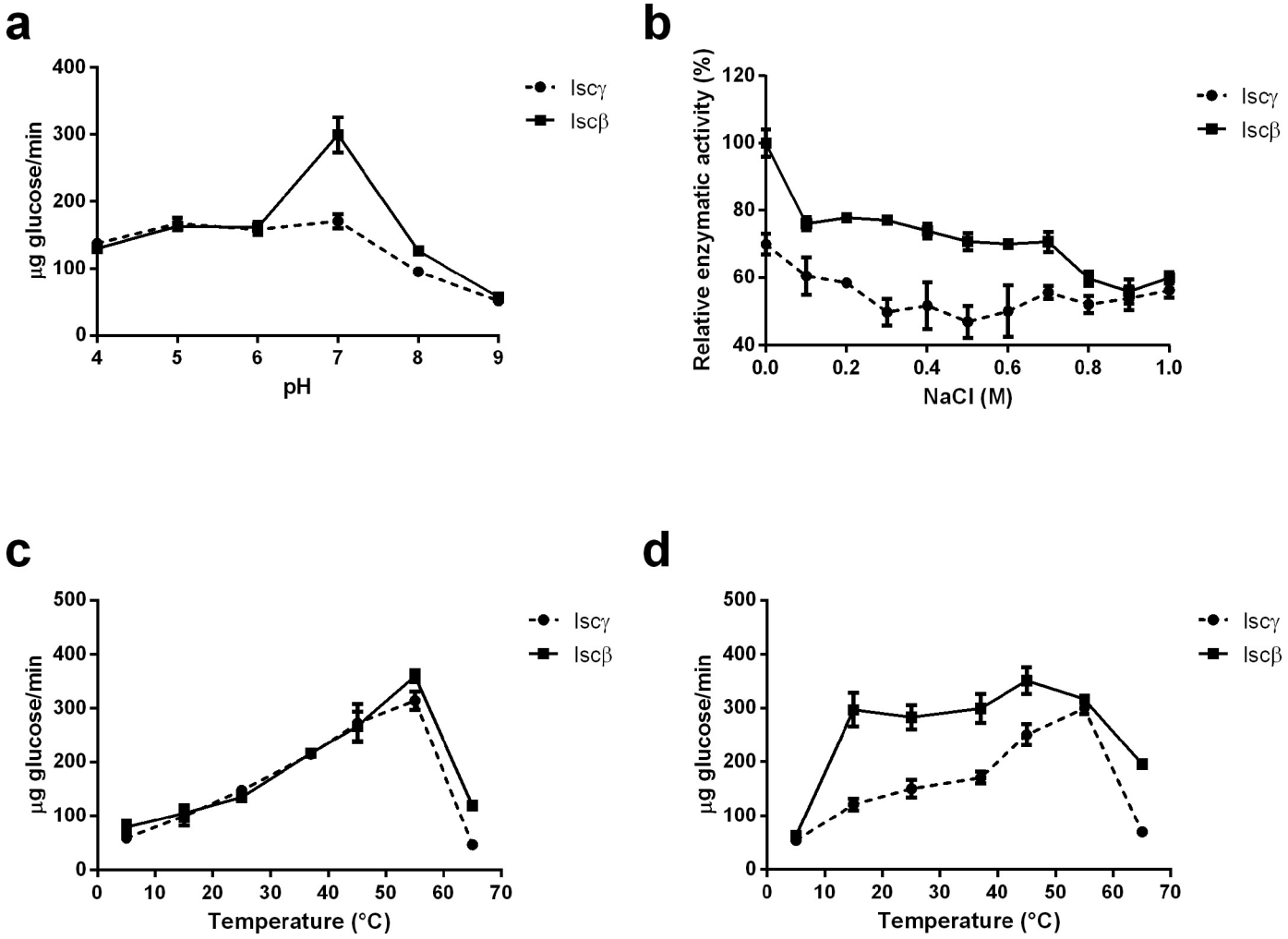

Fig. 4. Enzymatic activity of lscβ and lscγ: Influence of a) pH, b) ionic strength, c) and d) temperature on lscβ and lscγ activity. In c) the experiment was performed at pH 5.0 while in d) at pH 7.0. Data are the mean and standard deviation of three different experiments.

37 °C with 600 mM of sucrose and equal amount of purified protein in reaction (10 μg per mL of reaction mixture), being the turbidity of the solution at 400 nm related to levan synthesis.

Results indicated that the ability of the proteins in levan synthesis at pH 5.0 were very different (Fig. 6a). In fact, in our experimental conditions, lscγ showed a great increase of levan polymerization with a peak at 600 min and then the absorbance steadily decreases by time. The kinetics of lscβ presented a different trend showing that the increase of absorbance at 400 nm was very weak and strongly retarded (1600 min) as compared to lscγ (600 min). Surprisingly, at pH 7.0 the activity of the two enzymes was very similar, both producing very small amounts of levan (Fig. 6b). Based on these results it appears that in Psa3 levan formation occurs mainly at pH 5.0. We repeated the same experiment in the presence of 1 mM EDTA obtaining similar results confirming that the different activity it isn't due to heavy metal ions contaminations (data not shown).

Biphasic kinetic observed with lscγ at pH 5.0 (Fig. 6a) suggests that the enzyme start to depolymerize levan once substrate is completely exhausted. To confirm this hypothesis, we performed a further experiment adding more sucrose when the maximum of the absorbance was reached (Fig. 6c). As expected, we observe that polymerization reaction restart and continue until a new plateau is reached. This result confirms that biphasic kinetic is due to ability of enzyme to depolymerize levan produced.

Finally, we quantified the relationship between the initial polymerization rate and sucrose concentration for both lscβ and lscγ at pH 5.0 (Fig. 6d). The polymerization rate of lscγ increased sharply in relation to sucrose concentration reaching the maximum at 100 mM sucrose, and then steadily decreased, suggesting a strong inhibition of its activity by the substrate. Again, the behaviour of lscβ was different: the velocity of this enzyme was constant regardless of sucrose concentration and always very low as compared to lscγ (about 30 times) with a maximum at 200 mM sucrose.

3.7. *Lscβ and lscγ showed differential expression in Psa*

Since we have demonstrated in this work either that lscβ or lscγ are two active enzymes present in Psa3 and possess strikingly different kinetics parameters, to acquire useful information on their role in the biology of the pathogen, we have investigated their expression during the different phases of bacterial growth.

A 100 mL NB culture was inoculated with 100 μL of 3.6×10^5 cfu/mL Psa3 solution and grown bacteria at 25 °C for 10 days under shaking. At different time point the *lscβ* and *lscγ* mRNA expression, the pH of culture and the bacterial total number were examined (Fig. 7). The cells growth curve obtained had the typical phases of microbial growth in culture: lag (0–4 h), exponential (4–24 h), stationary (24–48 h), and death (48–240 h) (Fig. 7a).

The initial pH of the culture was 6.9 and increased during all the experiment following the same phases of cells growth: an initial lag phase (0–8 h), a drastic increase (8–24 h) during which the value shifted from 6.9 to 7.8, a stationary phase (24–48 h) and a final phase (48–240 h)

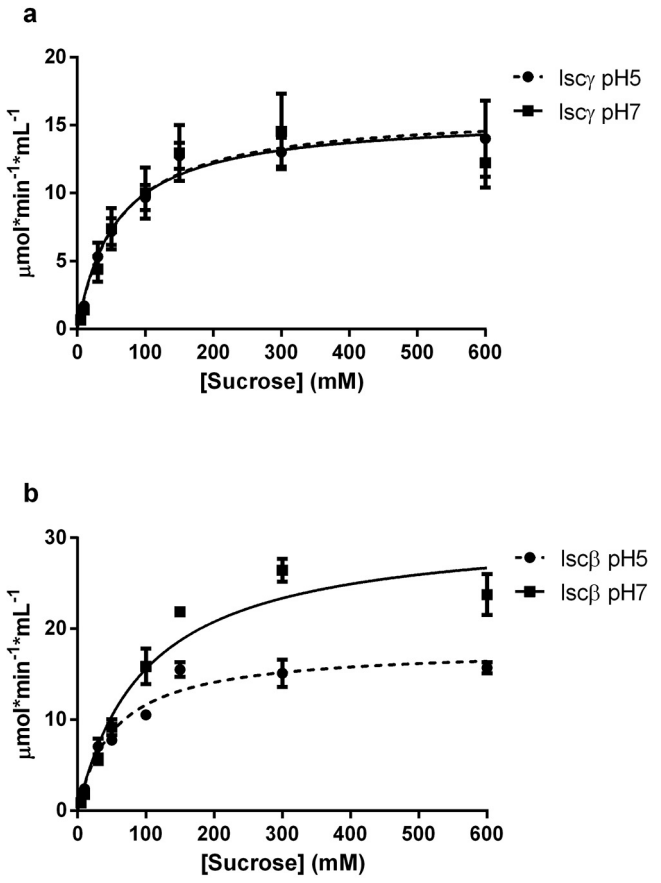

Fig. 5. Kinetic curves of lscβ and lscγ at different pH: a) Michaelis-Menten curves of lscγ at pH 5.0 and 7.0. b) Michaelis-Menten curves of lscβ at pH 5.0 and 7.0. Data are the mean and standard deviation of three different experiments.

during which the pH slowly albeit constantly increased to 8.9 (240 h, end of the experiment) (Fig. 7b). Based on this evidence, we can hypothesize that during growth Psa3KL103 secretes alkaline metabolites that basify the medium, as previously reported for other Pssc members [40,41].

To evaluate the *lscβ* and *lscγ* expressions during the time course pattern of the experiment, total RNA was extracted from cultivated bacteria, retro-transcribed to cDNA and analysed by qPCR method.

Results indicated that the expression level of *lscγ* did not change in a significant manner for all duration of the experiment (Fig. 7c). Differently, *lscβ* was expressed at similar level of *lscγ* just after inoculation of the growth medium, but after 24 h, the expression was increased 620 times (0 h = 0.04 ± 0.01 fg; 24 h = 24,80 ± 3,38 fg) and finally, returned sharply to the initial level. Interestingly, the 24 h time point coincided with the end of the exponential phase of bacterial growth, an event that is triggered by nutrients run out, rendering plausible to speculate that this enzyme is involved in response to nutrient deficiency as well as in a mechanism of negative feedback regulation, as the rapid return to the basal level suggests. In conclusion data here presented demonstrate that, at least *in vitro*, the two enzymes play a different role in the physiology of Psa3.

4. Discussion

The ability to produce EPSs confers a selective advantage to bacteria, whether plant pathogenic or not. During the epiphytic growth on the host plant, EPSs may help to form a biofilm matrix that holds the cells together, and them to attach to surfaces, that protects the cells from dehydration and favours cell to cell communication, carbon storage and protection from antimicrobial compounds [42,43]. On the other hand, during the parasitic growth of a bacterial pathogen, the EPSs could render possible for the parasite to avoid or delay the activation of plant defences [44,45]. Levan production is a common feature among members of the Pssc, which is useful for discriminating its members from other fluorescent plant pathogenic *Pseudomonas* when grown on sucrose rich media [1,29]. However the biological functions of levan for this vast group of plant pathogens is poorly understood and different hypotheses are currently under investigation: it can form a "barrier" on the bacterial cell that prevents recognition and consequent active responses by the host, as well as it can be a "side product" of the active release of glucose, the major carbon source for *P. syringae*, from sucrose, an abundant storage sugar present in the plant apoplast [19,46]. Here, we report the description of the enzymatic activity of two novel lscs, lscβ and lscγ, of Psa3 the causal agent of the current pandemic of canker disease of kiwifruit. Like other *P. syringae*, *e.g. P. syringae* pv. glycinea [20] and *P. syringae* pv. tomato [47] Psa3 it possesses at least three *lsc* genes. In particular, two are chromosome located (*lscα* and *lscβ*) while one is plasmid borne (*lscγ*). We found that the *lscα* sequence possess a G to A transition in position 187 that, by inducing the formation of a stop codon, probably makes the allele non-functional in this Psa lineage. Interestingly the presence of a likely non-functional *lscA* gene has also been described in *P. syringae* pv. glycinea PG 4180 due to an altered upstream region which does not seem to allow its expression [46]. Therefore, the levan production in Psa3 appears to relay on the sole *lscβ* and *lscγ* alleles. Moreover the first 14 predicted amino acids residues located at the putative N-terminus of the lscγ protein of Psa3, represent a unique motif among *P. syringae* levansucrases described so far [21]. Since previously characterized lscC and lscB from *P. syringae* pv glycinea are strikingly similar among each other at the amino acid level differing in only five residues [48], we decided to characterize this novel enzyme also by means of comparison to the other putatively functional lsc enzyme found in Psa3 KL103, lscβ.

To the aim, lscβ and lscγ gene were heterologously cloned and the recombinant proteins were expressed and purified for structural and kinetic studies. Indeed, from the structural point of view, the two Psa3 proteins presented similar CD spectra, analogue to other levansucrases, and compatible with their characteristic five-bladed β-propeller architecture [24]. Again, like several lscs [24], lscβ and lscγ enzymes exist in solution in a dimeric form and are highly thermostable with a T_m of 60.0 °C and 55.0 °C, respectively. On the other hand, we found that they behave very differently at enzymatic level, both in terms of sucrose splitting activity and levan synthesis.

In our experimental conditions, the amount of glucose (sucrose splitting) released by lscβ was double compared to lscγ at pH 7.0, while at pH 5.0 the two enzymes showed the same activity. The

Table 1
Biochemical characteristics of sucrose catalysis for recombinant levansucrases proteins of *P. syringae* pv. actinidiae at different pH.

Levansucrase protein	pH	Kinetic parameters		
		K_m (M)	k_{cat} (min^{-1})	k_{cat}/K_m (M^{-1} min^{-1})
lscβ	5	0.0541 ± 0.0093	$8,5 * 10^3$	$1,6 * 10^5$
lscβ	7	0.1001 ± 0.0201	$1,5 * 10^4$	$1,5 * 10^5$
lscγ	5	0.0604 ± 0.0090	$7,3 * 10^3$	$1,3 * 10^5$
lscγ	7	0.0573 ± 0.0138	$7,5 * 10^3$	$1,3 * 10^5$

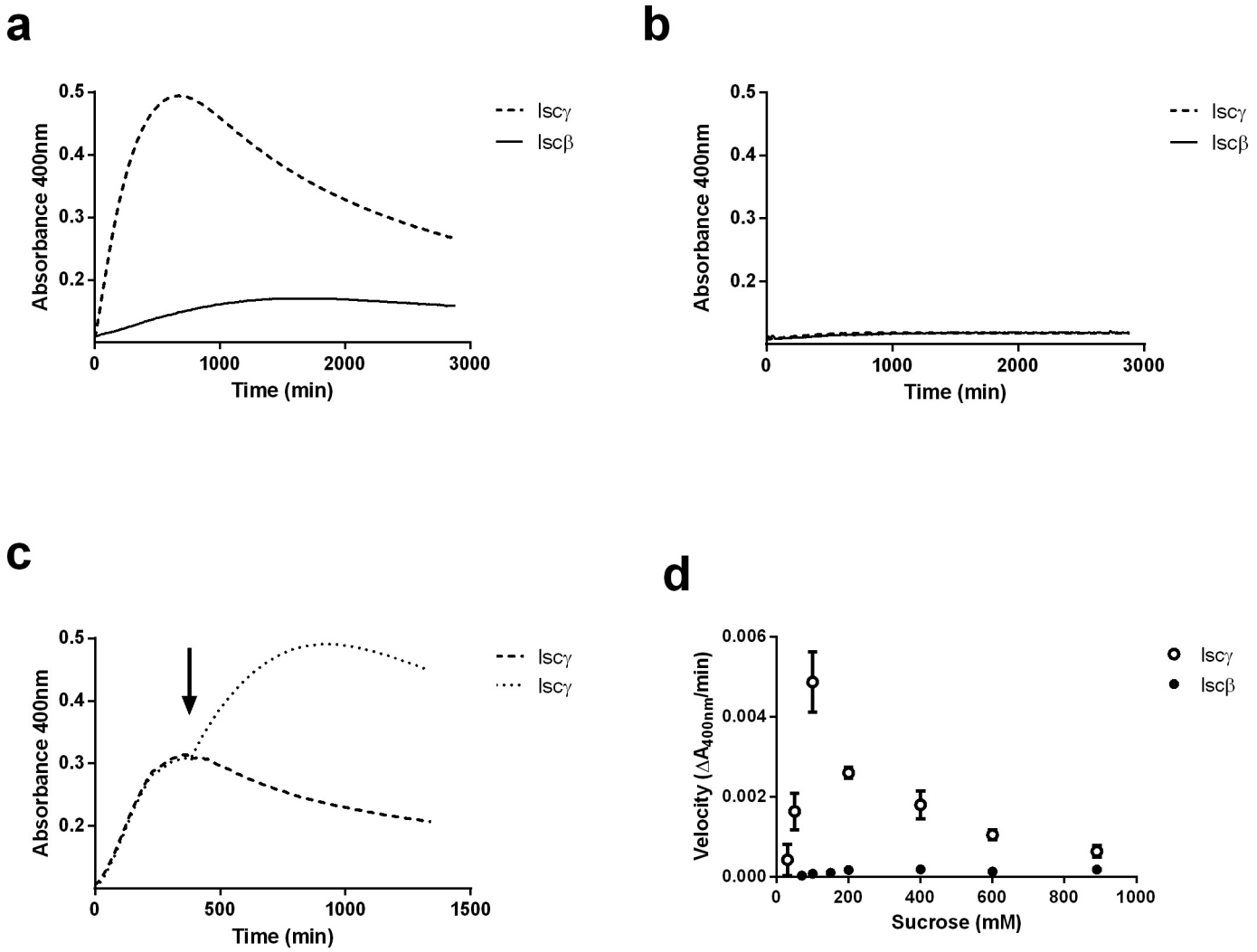

Fig. 6. Levan synthesis of lscβ and lscγ: a) time course of levan polymerization by lscβ and lscγ with 600 mM sucrose at pH 5.0 or b) pH 7.0. c) Levan polymerization by lscγ at pH 5.0 with 200 mM sucrose. Arrow indicated the further adding of 200 mM sucrose. d) Sucrose effect on lscβ and lscγ polymerization velocity at pH 5.0. Data are the mean and standard deviation of three different experiments.

differences in sucrose splitting were further corroborated by the kinetic parameter K_m and k_{cat} of the two enzymes at these pHs, albeit the K_m and k_{cat} that we registered are comparable to those of other characterized lscs [16,23]. Interestingly, we have found that in the case of lscβ but not in that of lscγ, the K_m e k_{cat} changes are clearly pH-dependent. In a similar manner, temperature and ionic strength, act differently on Psa3 lscβ and lscγ: lscβ is little susceptible to temperature changes but more sensitive to ionic strength meanwhile for lscγ the opposite is true. At last also the ability of lscβ and lscγ to synthetize levan was proven to be variably affected by different reaction conditions, with lscγ able to synthesize levan more quickly and in higher amounts at pH 5.0 but not at pH 7.0 at which the two enzymes synthesize levan in the same manner albeit at lower rates and amounts. Based on the results here presented, it could be then speculated that the two lsc isoforms found in Psa3, absolve to different functions under the same environmental conditions. Already Li and Ullrich in 2001 [20], had assumed that the redundancy of *lsc* genes in *P. syringae* might hint at different functions for each of the gene products, but, to the best of our knowledge, it has never been proven until now [16,21]. Remarkably, the *Zymomonas mobilis* lsc can exist in two different active forms depending on pH: at pH values above 7.0 the protein is a dimer with mainly sucrose hydrolysis activity, whereas at pH values below 6.0, the protein assembles spontaneously to ordered filaments and filamentous networks that are biologically active and specialized in levan synthesis, suggesting that at lower pH values, polymer synthesis is more important for the carrier strains [49]. If this is so, it could be expected that the different environmental conditions experienced by Psa3 KL103 induce a differential expression of the two *lsc* genes. To the aim, we carried out a very simple experiment, culturing Psa3 KL103 on NB at a constant temperature of 28 °C, that enabled us to show that, at least under *in vitro* conditions, *lscβ* was highly expressed at the end of the exponential phase of bacterial growth, while, in the same conditions, *lscγ* was not. To prove a differential gene expression between *lsc* isoforms in Psa3, is of particular interest given the fact that until now this measurement had been hindered for *P. syringae* because of the nearly identical gene sequence of *lsc* genes [20,21]. Whatsoever it is possible that in our *in vitro* experiment we were not able to recreate the conditions in terms of pH for *lscγ* gene expression since we have noticed that levan synthesis by lscγ enzyme occurs at pH 5.0, a condition at which Psa3KL103 does not grow on artificial media. Nnevertheless under *in vivo* conditions the multiplication of the pathogen under this pH value seems plausible.

It is well known that *P. syringae* exploits stomatal openings and wounds to entry in plants apoplast which presents an acidic pH (from 5.0 to 5.5) and thereafter a complex sequence of events, mediated by the infection process, activates a K^+/H^+ plant-borne efflux and influx, which increases the apoplastic pH to 7.5 [46]. Indeed Atkinson in 1987 [50] demonstrated that *P. syringae* pv. syringae multiplication in *Phaseolus vulgaris* is correlated with the increasing pH of host

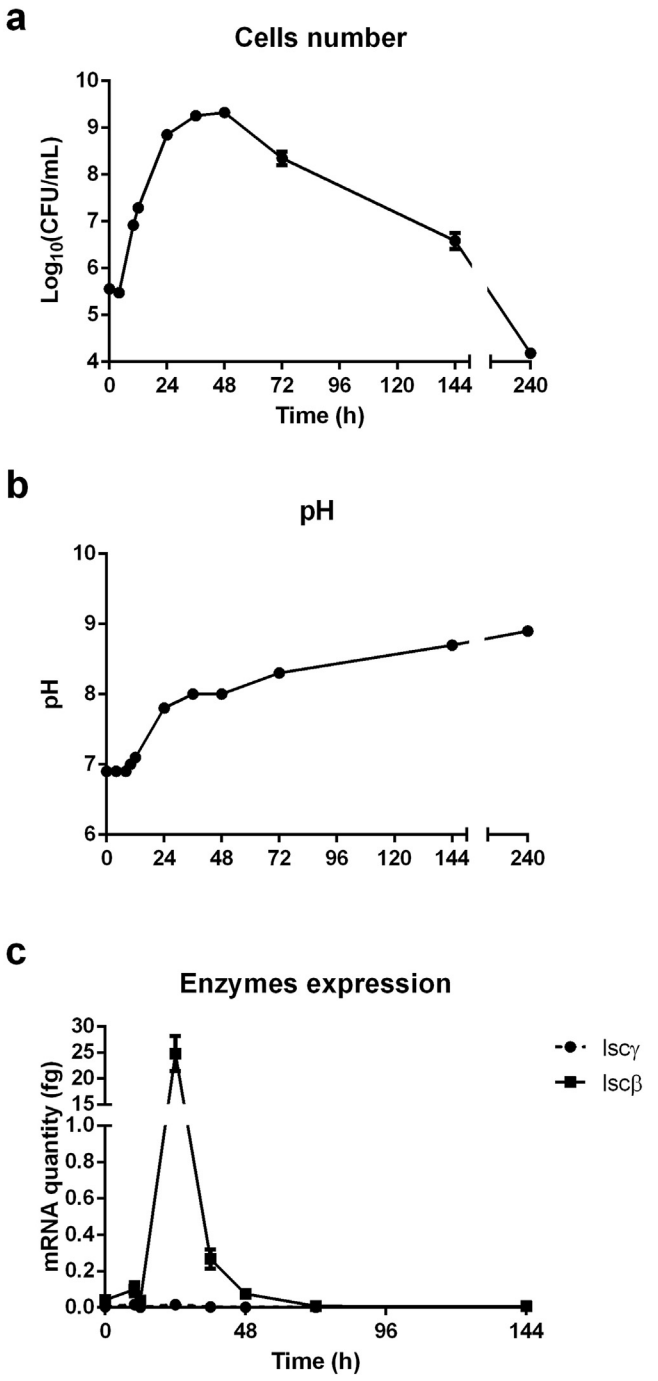

Fig. 7. *lscβ* and *lscγ* gene expressions: a) Quantifications of Psa3 cells number during bacterial growth. b) pH values measured during bacterial growth. c) Absolute quantification of *lscβ* and *lscγ* mRNA in Psa3 during bacterial growth. Data are the mean and standard deviation of three different experiments.

intercellular fluid resulting from the K^+/H^+ exchange. Taking into account that the 150 mM sucrose concentration used in our experiments is the sucrose quantity in the guard cells apoplast under photosynthetic conditions [51] and that stomata are a common port of entry for Psa [6,52], it becomes easy to speculate that the two active isoforms of Psa3 lscs here characterized could have different functions during the infection process of *Actinidia* spp. Since one of the first line of plant defence is to remove sucrose availability for pathogens [53], then lscγ could facilitate pathogen early stages of process (biotrophic phase), when the quick polymerization of levan would allow the bacterium to mask and protect itself providing at the same time a form of nutrient storage [18], at a higher pH value, lscβ would accelerate pathogen multiplication (necrotrophic phase) by producing large quantities of glucose for metabolism [54].

Further investigations are compelling to elucidate the role of the two enzymes in relation to pH changes, as well as in relation to temperature, a factor that had been recently proven to affected leaf colonization process of *Actinidia* spp. by Psa3 [55]. In fact, our data also indicated that the hydrolytic activity of lscβ was always near to its maximum at all temperatures tested while lscγ did not.

Apart from the phytopathological considerations, lsc exhibit great potential in food and pharmaceutical industries, in fact, levan has several applications such as nondigestible soluble dietary fiber and prebiotic compound or as drug showing antiobesity, antioxidant and antitumor effect [56]. The results obtained in the present study showed that lscγ is a highly stable levan producing protein at pH 5.0 and represent a good candidate for industrial application. In addition, future experiment highlighting the structural differences between lscβ and lscγ could reveal the key aminoacids that promote polymerization or hydrolysis. It has not escaped our notice that hydrolysis and transfructosylation reactions of lsc could be catalysed on different parts of the protein. Lscβ and lscγ enzymes share a 94.6% of identity at amino acid level. Since 14 out of 23 different positions are located at the N-terminal region, it will be of sure interest to investigate whether or not this region is responsible for the observed different behaviour in sucrose/polymer binding between the two enzymes, under different pH conditions. At last, also the comparison of the k_{cat} and K_m supports the existence of two different enzymes in Psa3, whose activity, under the same conditions, markedly differs both in terms of affinity for the substrate (K_m) and of catalytic activity (k_{cat}).

To the best of our knowledge, this is the first report with experimental evidence highlighting the possible different localization of the hydrolysis and transfructosylation reactions in lsc which till now were only supposed by molecular modelling [57].

Supplementary data to this article can be found online at https://doi.org/10.1016/j.ijbiomac.2021.02.189.

Funding

This study was supported by the University of Florence (Fondi di Ateneo 2019 e 2020) and the Phytosanitary Service of the Tuscany Region.

CRediT authorship contribution statement

Simone Luti: Conceptualization; Data curation; Investigation; Writing - original draft. **Sara Campigli**: Investigation; Methodology; Data curation; Writing, review & editing. **Francesco Ranaldi**: Methodology; Formal analysis; Writing, review & editing. **Paolo Paoli**: Validation; Visualization; Writing, review & editing. **Luigia Pazzagli**: Funding acquisition; Resources; Writing, review & editing. **Guido Marchi:** Conceptualization; Resources; Funding acquisition; Supervision; Writing, review & editing.

Acknowledgements

Dr. Simone Luti and Dr. Sara Campigli were financed by a grant from the Phytosanitary Service of the Tuscany Region and the University of Florence (Italy). We are grateful to Dr. Costanza Cicchi for her contribution in sucrose hydrolysis experiments during her bachelor's degree Thesis and Dr. Domenico Rizzo for feedback on the manuscript.

The authors declare no conflict of interest.

References

[1] L. Gardan, C. Bollet, M. Abu Ghorrah, F. Grimont, P.A.D. Grimont, DNA relatedness among the pathovar strains of Pseudomonas syringae subsp. savastanoi Janse (1982) and proposal of Pseudomonas savastanoi sp. nov, Int. J. Syst. Bacteriol. 42 (1992) 606–612, https://doi.org/10.1099/00207713-42-4-606.

[2] T. Fujikawa, H. Sawada, Genome analysis of the kiwifruit canker pathogen Pseudomonas syringae pv. actinidiae biovar 5, Sci. Rep. 6 (2016), 21399, https://doi.org/10.1038/srep21399.
[3] J.R. Chapman, R.K. Taylor, B.S. Weir, M.K. Romberg, J.L. Vanneste, J. Luck, B.J.R. Alexander, Phylogenetic relationships among global populations of Pseudomonas syringae pv. actinidiae, Phytopathology® 102 (2012) 1034–1044, https://doi.org/10.1094/PHYTO-03-12-0064-R.
[4] H. Sawada, T. Miyoshi, Y. Ide, Novel MLSA group (Psa5) of Pseudomonas syringae pv. actinidiae causing bacterial canker of kiwifruit (Actinidia chinensis) in Japan, Japanese Journal of Phytopathology 80 (2014) 171–184, https://doi.org/10.3186/jjphytopath.80.171.
[5] A. Cunty, F. Poliakoff, C. Rivoal, S. Cesbron, M. Fischer-Le Saux, C. Lemaire, M.A. Jacques, C. Manceau, J.L. Vanneste, Characterization of Pseudomonas syringae pv. actinidiae (Psa) isolated from France and assignment of Psa biovar 4 to a de novo pathovar: Pseudomonas syringae pv. actinidifoliorum pv. nov, Plant Pathol. 64 (2015) 582–596, https://doi.org/10.1111/ppa.12297.
[6] J.L. Vanneste, The scientific, economic, and social impacts of the New Zealand outbreak of bacterial canker of kiwifruit (Pseudomonas syringae pv. actinidiae), Annu. Rev. Phytopathol. 55 (2017) 377–399, https://doi.org/10.1146/annurev-phyto-080516-035530.
[7] H.C. Mccann, E.H.A. Rikkerink, F. Bertels, M. Fiers, A. Lu, J. Rees-George, M.T. Andersen, A.P. Gleave, B. Haubold, M.W. Wohlers, D.S. Guttman, P.W. Wang, C. Straub, J. Vanneste, P.B. Rainey, M.D. Templeton, Genomic analysis of the kiwifruit pathogen Pseudomonas syringae pv. actinidiae provides insight into the origins of an emergent plant disease, PLoS Pathog. 9 (2013), e1003503, https://doi.org/10.1371/journal.ppat.1003503.
[8] H. Sawada, S. Shimizu, T. Miyoshi, T. Shinozaki, S. Kusumoto, M. Noguchi, T. Naridomi, K. Kikuhara, M. Kansako, T. Fujikawa, R. Nakaune, Characterization of biovar 3 strains of Pseudomonas syringae pv. Actinidiae isolated in Japan, Japanese Journal of Phytopathology 81 (2015) 111–126, https://doi.org/10.3186/jjphytopath.81.111.
[9] P. Petrova, K. Petrov, Lactic acid fermentation of cereals and pseudocereals: ancient nutritional biotechnologies with modern applications, Nutrients 12 (2020) 1118, https://doi.org/10.3390/nu12041118.
[10] A. Lovato, A. Pignatti, N. Vitulo, E. Vandelle, A. Polverari, Inhibition of virulence-related traits in Pseudomonas syringae pv. actinidiae by gunpowder green tea extracts, Front. Microbiol. 10 (2019)https://doi.org/10.3389/fmicb.2019.02362.
[11] P.A. Mcatee, L. Brian, B. Curran, O. van der Linden, N.J. Nieuwenhuizen, X. Chen, R.A. Henry-Kirk, E.A. Stroud, S. Nardozza, J. Jayaraman, E.H.A. Rikkerink, C.G. Print, A.C. Allan, M.D. Templeton, Re-programming of Pseudomonas syringae pv. actinidiae gene expression during early stages of infection of kiwifruit, BMC Genomics 19 (2018), 822, https://doi.org/10.1186/s12864-018-5197-5.
[12] S.P. Kidambi, G.W. Sundin, D.A. Palmer, A.M. Chakrabarty, C.L. Bender, Copper as a signal for alginate synthesis in Pseudomonas syringae pv. syringae, Appl. Environ. Microbiol. 61 (1995) 2172–2179, https://doi.org/10.1128/AEM.61.6.2172-2179.1995.
[13] J. Yu, A. Penaloza-Vazquez, A.M. Chakrabarty, C.L. Bender, Involvement of the exopolysaccharide alginate in the virulence and epiphytic fitness of Pseudomonas syringae pv. syringae, Mol. Microbiol. 33 (1999) 712–720, https://doi.org/10.1046/j.1365-2958.1999.01516.x.
[14] R.C. Keith, L.M.W. Keith, G. Hernández-Guzmán, S.R. Uppalapati, C.L. Bender, Alginate gene expression by Pseudomonas syringae pv. tomato DC3000 in host and non-host plants, Microbiology 149 (2003) 1127–1138, https://doi.org/10.1099/mic.0.26109-0.
[15] T.C. Helmann, A.M. Deutschbauer, S.E. Lindow, Genome-wide identification of Pseudomonas syringae genes required for fitness during colonization of the leaf surface and apoplast, Proc. Natl. Acad. Sci. 116 (2019) 18900–18910, https://doi.org/10.1073/pnas.1908858116.
[16] E.T. Öner, L. Hernández, J. Combie, Review of Levan polysaccharide: from a century of past experiences to future prospects, Biotechnol. Adv. 34 (2016) 827–844, https://doi.org/10.1016/j.biotechadv.2016.05.002.
[17] P. Bogino, M. Oliva, F. Sorroche, W. Giordano, The role of bacterial biofilms and surface components in plant-bacterial associations, Int. J. Mol. Sci. 14 (2013) 15838–15859, https://doi.org/10.3390/ijms140815838.
[18] H. Laue, A. Schenk, H. Li, L. Lambertsen, T.R. Neu, S. Molin, M.S. Ullrich, Contribution of alginate and levan production to biofilm formation by Pseudomonas syringae, Microbiology 152 (2006) 2909–2918, https://doi.org/10.1099/mic.0.28875-0.
[19] S. Kasapis, E.R. Morris, M. Gross, K. Rudolph, Solution properties of levan polysaccharide from Pseudomonas syringae pv. phaseolicola, and its possible primary role as a blocker of recognition during pathogenesis, Carbohydr. Polym. 23 (1994) 55–64, https://doi.org/10.1016/0144-8617(94)90090-6.
[20] H. Li, M.S. Ullrich, Characterization and mutational analysis of three allelic lsc genes encoding levansucrase in Pseudomonas syringae, J. Bacteriol. 183 (2001) 3282–3292, https://doi.org/10.1128/JB.183.11.3282-3292.2001.
[21] A. Srivastava, N. Al-Karablieh, S. Khandekar, A. Sharmin, H. Weingart, M.S. Ullrich, Genomic distribution and divergence of levansucrase-coding genes in Pseudomonas syringae, Genes 3 (2012) 115–137, https://doi.org/10.3390/genes3010115.
[22] T. Visnapuu, K. Mardo, C. Mosoarca, A.D. Zamfir, A. Vigants, T. Alamäe, Levansucrases from Pseudomonas syringae pv. tomato and P. chlororaphis subsp. aurantiaca: substrate specificity, polymerizing properties and usage of different acceptors for fructosylation, J. Biotechnol. 155 (2011) 338–349, https://doi.org/10.1016/j.jbiotec.2011.07.026.
[23] T. Visnapuu, K. Mardo, T. Alamäe, Levansucrases of a Pseudomonas syringae pathovar as catalysts for the synthesis of potentially prebiotic oligo- and polysaccharides, New Biotechnol. 32 (2015) 597–605, https://doi.org/10.1016/j.nbt.2015.01.009.
[24] M.E. Ortiz-Soto, J.R. Porras-Domínguez, J. Seibel, A. López-Munguía, A close look at the structural features and reaction conditions that modulate the synthesis of low and high molecular weight fructans by levansucrases, Carbohydr. Polym. 219 (2019) 130–142, https://doi.org/10.1016/j.carbpol.2019.05.014.
[25] K. Mardo, T. Visnapuu, H. Vija, T. Elmi, T. Alamäe, Mutational analysis of conserved regions harboring catalytic triad residues of the levansucrase protein encoded by the lsc-3 gene (lsc3) of Pseudomonas syringae pv. tomato DC3000, Biotechnol. Appl. Biochem. 61 (2014) 11–22, https://doi.org/10.1002/bab.1129.
[26] G. Rabbani, E. Ahmad, N. Zaidi, R.H. Khan, pH-dependent conformational transitions in conalbumin (ovotransferrin), a metalloproteinase from hen egg white, Cell Biochem. Biophys. 61 (2011) 551–560, https://doi.org/10.1007/s12013-011-9237-x.
[27] W. Xu, D. Ni, W. Zhang, C. Guang, T. Zhang, W. Mu, Recent advances in levansucrase and inulosucrase: evolution, characteristics, and application, Crit. Rev. Food Sci. Nutr. 59 (2019) 3630–3647, https://doi.org/10.1080/10408398.2018.1506421.
[28] S.K. Mohan, An improved agar plating assay for detecting Pseudomonas syringae pv. syringae and P. s. pv. Phaseolicola in contaminated bean seed, Phytopathology 77 (1987) 1390, https://doi.org/10.1094/Phyto-77-1390.
[29] R.A. Lelliott, E. Billing, A.C. Hayward, A determinative scheme for the fluorescent plant pathogenic pseudomonads, J. Appl. Bacteriol. 29 (1966) 470–489, https://doi.org/10.1111/j.1365-2672.1966.tb03499.x.
[30] S. Kumar, G. Stecher, M. Li, C. Knyaz, K. Tamura, MEGA X: molecular evolutionary genetics analysis across computing platforms, Mol. Biol. Evol. 35 (2018) 1547–1549, https://doi.org/10.1093/molbev/msy096.
[31] M.V. Vega, A. Nigro, S. Luti, C. Capitini, G. Fani, L. Gonnelli, F. Boscaro, F. Chiti, Isolation and characterization of soluble human full-length TDP-43 associated with neurodegeneration, FASEB J. 33 (2019) 10780–10793, https://doi.org/10.1096/fj.201900474R.
[32] G. Rabbani, E. Ahmad, M.V. Khan, M.T. Ashraf, R. Bhat, R.H. Khan, Impact of structural stability of cold adapted Candida antarctica lipase B (CaLB): in relation to pH, chemical and thermal denaturation, RSC Adv. 5 (2015) 20115–20131, https://doi.org/10.1039/C4RA17093H.
[33] A. El Khatib, Practical biochemistry principles and techniques approach, Progress in Chemical and Biochemical Research 3 (2020) 180–193.
[34] C. Gonçalves, R.M. Rodriguez-Jasso, N. Gomes, J.A. Teixeira, I. Belo, Adaptation of dinitrosalicylic acid method to microtiter plates, Anal. Methods 2 (2010) 2046, https://doi.org/10.1039/c0ay00525h.
[35] H.C. Ball, R.K. Holmes, R.L. Londraville, J.G.M. Thewissen, R.J. Duff, Leptin in whales: validation and measurement of mRNA expression by absolute quantitative real-time PCR, PLoS One 8 (2013), e54277, https://doi.org/10.1371/journal.pone.0054277.
[36] R.T.M. Poulter, J. Ho, T. Handley, G. Taiaroa, M.I. Butler, Comparison between complete genomes of an isolate of Pseudomonas syringae pv. actinidiae from Japan and a New Zealand isolate of the pandemic lineage, Sci. Rep. 8 (2018), 10915, https://doi.org/10.1038/s41598-018-29261-5.
[37] B. Caroline, M. Goncalves, C. Baldo, M. Antonia, P. Colabone, Levan And Levansucrase-A Mini Review, Int. J. Sci. Technol. Res. 4 (2015) 100–104.
[38] A. Mukherjee, S. Banerjee, R. Gachhui, Investigation of conformational changes of levansucrase isolated from Acetobacter nitrogenifigens strain RG1 by mercuric and cadmium ion, Int. J. Biol. Macromol. 120 (2018) 189–194, https://doi.org/10.1016/j.ijbiomac.2018.08.083.
[39] G. Rabbani, I. Choi, Roles of osmolytes in protein folding and aggregation in cells and their biotechnological applications, Int. J. Biol. Macromol. 109 (2018) 483–491, https://doi.org/10.1016/j.ijbiomac.2017.12.100.
[40] M.A.P. Manzoor, S.R. Duwal, M. Mujeeburahiman, P.-D. Rekha, Vitamin C inhibits crystallization of struvite from artificial urine in the presence of Pseudomonas aeruginosa, International Braz j Urol 44 (2018) 1234–1242, https://doi.org/10.1590/s1677-5538.ibju.2017.0656.
[41] D.R. Kurnia, W. Mangunwardoyo, H. Ambarsari, Biodegradation of used lubricant oil hydrocarbons using Bacillus subtilis InaCC B289 and *Pseudomonas aeruginosa* InaCC B290 in single or mixed cultures, 2018 070007, https://doi.org/10.1063/1.5062805.
[42] S. Tsuneda, H. Aikawa, H. Hayashi, A. Yuasa, A. Hirata, Extracellular polymeric substances responsible for bacterial adhesion onto solid surface, FEMS Microbiol. Lett. 223 (2003) 287–292, https://doi.org/10.1016/S0378-1097(03)00399-9.
[43] O.Y.A. Costa, J.M. Raaijmakers, E.E. Kuramae, Microbial extracellular polymeric substances: ecological function and impact on soil aggregation, Front. Microbiol. 9 (2018)https://doi.org/10.3389/fmicb.2018.01636.
[44] Z. Király, H.M. El-Zahaby, Z. Klement, Role of extracellular polysaccharide (EPS) slime of plant pathogenic bacteria in protecting cells to reactive oxygen species, J. Phytopathol. 145 (1997) 59–68, https://doi.org/10.1111/j.1439-0434.1997.tb00365.x.
[45] M.C. de Pinto, P. Lavermicocca, A. Evidente, M.M. Corsaro, S. Lazzaroni, L. De Gara, Exopolysaccharides produced by plant pathogenic bacteria affect ascorbate metabolism in Nicotiana tabacum, Plant Cell Physiol. 44 (2003) 803–810, https://doi.org/10.1093/pcp/pcg105.
[46] A. Mehmood, K. Abdallah, S. Khandekar, D. Zhurina, A. Srivastava, N. Al-Karablieh, G. Alfaro-Espinoza, D. Pletzer, M.S. Ullrich, Expression of extra-cellular levansucrase in Pseudomonas syringae is controlled by the in planta fitness-promoting metabolic repressor HexR, BMC Microbiol. 15 (2015) 48, https://doi.org/10.1186/s12866-015-0349-0.
[47] T. Visnapuu, A. Mäe, T. Alamäe, Hansenula polymorpha maltase gene promoter with sigma 70-like elements is feasible for Escherichia coli-based biotechnological applications: expression of three genomic levansucrase genes of Pseudomonas syringae pv. tomato, Process Biochem. 43 (2008) 414–422, https://doi.org/10.1016/j.procbio.2008.01.002.
[48] H. Li, A. Schenk, A. Srivastava, D. Zhurina, M.S. Ullrich, Thermo-responsive expression and differential secretion of the extracellular enzyme levansucrase in the plant pathogenic bacterium Pseudomonas syringae pv. glycinea, FEMS Microbiol. Lett. 265 (2006) 178–185, https://doi.org/10.1111/j.1574-6968.2006.00486.x.

[49] D. Goldman, N. Lavid, A. Schwartz, G. Shoham, D. Danino, Y. Shoham, Two active forms of Zymomonas mobilis levansucrase, J. Biol. Chem. 283 (2008) 32209–32217, https://doi.org/10.1074/jbc.M805985200.
[50] M.M. Atkinson, Association of host plasma membrane K + /H + exchange with multiplication of Pseudomonas syringae pv. syringae in Phaseolus vulgaris, Phytopathology 77 (1987) 1273, https://doi.org/10.1094/Phyto-77-1273.
[51] Y. Kang, W.H. Outlaw, P.C. Andersen, G.B. Fiore, Guard-cell apoplastic sucrose concentration? A link between leaf photosynthesis and stomatal aperture size in the apoplastic phloem loader Vicia faba L, Plant Cell Environ. 30 (2007) 551–558, https://doi.org/10.1111/j.1365-3040.2007.01635.x.
[52] I. Donati, A. Cellini, D. Sangiorgio, J.L. Vanneste, M. Scortichini, G.M. Balestra, F. Spinelli, Pseudomonas syringae pv. actinidiae: ecology, infection dynamics and disease epidemiology, Microb. Ecol. 80 (2020) 81–102, https://doi.org/10.1007/s00248-019-01459-8.
[53] L.-Q. Chen, X.-Q. Qu, B.-H. Hou, D. Sosso, S. Osorio, A.R. Fernie, W.B. Frommer, Sucrose efflux mediated by SWEET proteins as a key step for phloem transport, Science 335 (2012) 207–211, https://doi.org/10.1126/science.1213351.
[54] M. Petriccione, A.M. Salzano, I. Di Cecco, A. Scaloni, M. Scortichini, Proteomic analysis of the Actinidia deliciosa leaf apoplast during biotrophic colonization by Pseudomonas syringae pv. actinidiae, J. Proteome 101 (2014) 43–62, https://doi.org/10.1016/j.jprot.2014.01.030.
[55] X. Gao, Q. Huang, Z. Zhao, Q. Han, X. Ke, H. Qin, L. Huang, Studies on the infection, colonization, and movement of Pseudomonas syringae pv. actinidiae in kiwifruit tissues using a GFPuv-labeled strain, PLoS One 11 (2016), e0151169, https://doi.org/10.1371/journal.pone.0151169.
[56] W. Li, S. Yu, T. Zhang, B. Jiang, W. Mu, Recent novel applications of levansucrases, Appl. Microbiol. Biotechnol. 99 (2015) 6959–6969, https://doi.org/10.1007/s00253-015-6797-5.
[57] B. Bakar, B. Kaplan-Türköz, Structural modelling and structure-function analysis of Zymomonas mobilis levansucrase, Süleyman Demirel Üniversitesi Fen Bilimleri Enstitüsü Dergisi 21 (2017) 279, https://doi.org/10.19113/sdufbed.81065.